

The Neuronal Ca²⁺ Sensor Protein Visinin-like Protein-1 Is Expressed in Pancreatic Islets and Regulates Insulin Secretion^{*[5]}

Received for publication, December 2, 2005, and in revised form, May 9, 2006. Published, JBC Papers in Press, May 26, 2006, DOI 10.1074/jbc.M512924200

Feihan F. Dai^{†1}, Yi Zhang[‡], Youhou Kang[‡], Qinghua Wang[‡], Herbert Y. Gaisano[‡], Karl-Heinz Braunewell[§], Catherine B. Chan[¶], and Michael B. Wheeler^{‡2}

From the [†]Departments of Physiology and Medicine, University of Toronto, Toronto, Ontario M5S 1A8, Canada, the [§]Signal Transduction Research Group, Neuroscience Research Center of the Charité, Universitätsmedizin Berlin, 10117 Berlin, Germany, and the [¶]Department of Biomedical Sciences, University of Prince Edward Island, Charlottetown, Prince Edward Island C1A 4P3, Canada

Visinin-like protein-1 (VILIP-1) is a member of the neuronal Ca²⁺ sensor protein family that modulates Ca²⁺-dependent cell signaling events. VILIP-1, which is expressed primarily in the brain, increases cAMP formation in neural cells by modulating adenylyl cyclase, but its functional role in other tissues remains largely unknown. In this study, we demonstrate that VILIP-1 is expressed in murine pancreatic islets and β -cells. To gain insight into the functions of VILIP-1 in β -cells, we used both overexpression and small interfering RNA knockdown strategies. Overexpression of VILIP-1 in the MIN6 β -cell line or isolated mouse islets had no effect on basal insulin secretion but significantly increased glucose-stimulated insulin secretion. cAMP accumulation was elevated in VILIP-1-overexpressing cells, and the protein kinase A inhibitor H-89 attenuated increased glucose-stimulated insulin secretion. Overexpression of VILIP-1 in isolated mouse β -cells increased cAMP content accompanied by increased cAMP-responsive element-binding protein gene expression and enhanced exocytosis as detected by cell capacitance measurements. Conversely, VILIP-1 knockdown by small interfering RNA caused a reduction in cAMP accumulation and produced a dramatic increase in preproinsulin mRNA, basal insulin secretion, and total cellular insulin content. The increase in preproinsulin mRNA in these cells was attributed to enhanced insulin gene transcription. Taken together, we have shown that VILIP-1 is expressed in pancreatic β -cells and modulates insulin secretion. Increased VILIP-1 enhanced insulin secretion in a cAMP-associated manner. Down-regulation of VILIP-1 was accompanied by decreased cAMP accumulation but increased insulin gene transcription.

Visinin-like protein-1 (VILIP-1)³ belongs to a family of neuronal Ca²⁺ sensor (NCS) proteins, which are conserved from yeast to human (1). The NCS family consists of ~40 members in different species divided into five subfamilies (1). Group III, the VILIP family, includes VILIP-1, VILIP-2, VILIP-3, hippocalcin, and neurocalcin- δ (1). NCS family members possess four EF-hand Ca²⁺-binding motifs. Calcium binding leads to a conformational change in the proteins, a mechanism termed the Ca²⁺-myristoyl switch, which facilitates their association with lipid bilayers (2). The NCS proteins are reported to have a variety of biological functions. These include involvement in the modulation of voltage-gated Ca²⁺ and A-type K⁺ channels (3, 4), transcriptional repression (5), kinase modulation (6), and neurotransmitter release (7, 8).

VILIP-1 was first cloned from a rat brain cDNA library (9), and at the protein level, it was shown to have 100% homology to human visinin-like peptide-1 (10). To date, studies on VILIP-1 have focused primarily on its role in neurons. Some of these studies have demonstrated Ca²⁺-dependent association with plasma membranes (11, 12) and Golgi membranes (12), which might be a mechanism for the coordinated regulation of signaling cascades. Furthermore, in a human embryonic kidney cell line (tsA201), VILIP-1 has been shown to increase cell-surface expression of α_4 - and β_2 -subunits of the neuronal nicotinic acetylcholine receptor, which belongs to a superfamily of ligand-gated ion channels (13). In addition, VILIP-1 has modulatory effects on signaling of cAMP and cGMP in neuronal and peripheral cells (11, 14–18). VILIP-1 has also been shown to increase cGMP levels in transfected C6 and PC12 cells by directly acting on guanylyl cyclase (17). Recent studies indicate that VILIP-1 modulates the activity of the receptor, guanylyl cyclase B, through clathrin-dependent receptor cycling, supporting a general physiological role for VILIP-1 in membrane trafficking within the central nervous system (14). In addition, VILIP-1 has been shown to bind double-stranded RNA as a protein-RNA complex for regulating the stability and localization

* This work was supported in part by an operating grant from the Canadian Diabetes Association (to M. B. W.) and Grant MOP-12898 from the Canadian Institutes of Health Research (to M. B. W. and C. B. C.). The costs of publication of this article were defrayed in part by the payment of page charges. This article must therefore be hereby marked "advertisement" in accordance with 18 U.S.C. Section 1734 solely to indicate this fact.

[5] The on-line version of this article (available at <http://www.jbc.org>) contains supplemental Figs. 1 and 2.

¹ Supported by New Emerging Teams Grant NET-54012 from the Canadian Institutes of Health Research.

² Recipient of a Canadian Institutes of Health Research investigator award. To whom correspondence should be addressed: Dept. of Physiology, University of Toronto, 1 King's College Circle, Toronto, Ontario M5S 1A8, Canada. Tel.: 416-978-6737; Fax: 416-978-4940; E-mail: michael.wheeler@utoronto.ca.

³ The abbreviations used are: VILIP-1, visinin-like protein-1; NCS, neuronal Ca²⁺ sensor; siRNA, small interfering RNA; EGFP, enhanced green fluorescent protein; Ad, adenovirus; GSIS, glucose-stimulated insulin secretion; GST, glutathione S-transferase; PKA, protein kinase A; RRP, readily releasable pool; RP, reserve pool; ff, femtofarads; CREB, cAMP-responsive element-binding protein.

tion of specific mRNAs, implicating its role in the regulation of gene expression (19).

VILIP-1 is expressed primarily in the brain, but lower expression has also been found in some peripheral organs, including the heart, testes, ovaries, and colon (20). Although many studies have reported on the biological functions of VILIP-1 in neurons, very little information is available regarding physiological roles in other tissues. In MIN6 cells, however, expression profiling of fatty acid-responsive genes has shown that oleic acid can significantly induce expression of VILIP-1 (21). In this study, we identified VILIP-1 in mouse pancreatic islets, and using overexpression and small interfering RNA (siRNA) knockdown strategies, we determined that VILIP-1 can regulate insulin secretion and insulin gene transcription. This study provides the first evidence that VILIP-1 plays a functional role in pancreatic β -cells.

MATERIALS AND METHODS

Reagents—The polyclonal antibody to VILIP-1 (rabbit anti-serum) and the vector harboring the full-length cDNA of VILIP-1 or the fusion protein VILIP-1-enhanced green fluorescent protein (EGFP) have been described previously (12, 15). Vectors expressing SNAP25 (synaptosome-associated protein of 25 kDa) and syntaxin-1A in mammalian cells were described in previous studies (22, 23). The constructs of firefly luciferase driven by the rat insulin I promoter and *Renilla* luciferase driven by the cytomegalovirus promoter were gifts from Dr. Donald Fleenor (Duke University). The vector expressing NCS-1 protein was kindly provided by Dr. John Roder (Samuel Lunenfeld Research Institute, Mount Sinai Hospital, Toronto). Bovine serum albumin, oleic acid, H-89, forskolin, ionomycin, collagenase V, dispase II, rabbit polyclonal antibody against β -actin, and mouse monoclonal antibodies against syntaxin-1A and SNAP25 were products of Sigma. Mouse monoclonal antibodies against cellular subfractionation marker proteins annexin II, caveolin-1, and lamin A/C were obtained from Clontech. Guinea pig anti-insulin and mouse anti-glucagon antibodies were from Dako. Fluorescein isothiocyanate- or Cy5-conjugated secondary antibody was from Jackson ImmunoResearch Laboratories, Inc. (West Grove, PA). Lipofectamine 2000, TRIzol, SuperScript II RNase H reverse transcriptase, ROX reference dye, SYBR Green dye, and Platinum *Taq* were purchased from Invitrogen. The cAMP assay kit was obtained from Biomedical Technologies, Inc. (Stoughton, MA). The Dual-Luciferase reporter assay kit was from Promega Corp. (Madison, WI). The siRNA duplex was designed using the program provided by Integrated DNA Technologies, Inc. (Coralville, IA), and the synthesis and high pressure liquid chromatography purification of the siRNAs were performed by the same company. The fluorescein-conjugated scrambled siRNA was from Dharmacon, Inc. (Lafayette, CO). The Qproteome compartment kit was purchased from Qiagen Inc.

Cell Culture—MIN6 cells (a gift from Dr. S. Seino, Chiba University), α -TC6 cells (kindly provided by Dr. Y. Moriyama, Okayama University), and HEK293 cells (purchased from American Type Culture Collection, Manassas, VA) were grown in monolayers in Dulbecco's modified Eagle's medium contain-

ing 25 mM glucose supplemented with 10% fetal bovine serum, 100 units/ml penicillin, and 100 μ g/ml streptomycin at 37 °C in a humidified atmosphere (5% CO₂). Cells were passaged every 4–5 days at 80% confluence.

Mouse Islet Isolation and Treatment—Mouse islets were isolated from male FVB/N mice (~2 months of age) as described previously (24). To obtain single islet cells, these intact mouse islets were dispersed in dispase II solution (0.6–2.4 units/ml) for 5 min and loaded onto glass coverslips after being washed with culture medium. The intact islets and single islet cells were cultured in RPMI 1640 medium containing 11.1 mM glucose supplemented with 10% fetal bovine serum, 10 mM HEPES, 100 units/ml penicillin, and 100 μ g/ml streptomycin for 24 h before being assayed.

Construction and Expression of siRNAs, Viruses, and Plasmids—The sequences of the siRNA duplex targeted to VILIP-1 were 5'-GAACAAAGAUGACCAGAUUTT-3' (sense) and 5'-AAUCUGGUCAUCUUGUUCTT-3' (antisense), corresponding to nucleotides 480–498 of mouse VILIP-1 cDNA (GenBankTM accession number D21165). The oligonucleotide sequences were subjected to a BLAST search, and no significant identity to other sequences was detected. The scrambled nonsense siRNA duplex sequences used as a negative control in MIN6 cells were 5'-UCAGAGUCUCGCAAUCACGTT-3' (sense) and 5'-CGUGAUUGCGAGACUCUGATT-3' (antisense) as described (25). The control duplex showed no significant homology to any known protein as assessed using the BLAST and NCBI Databases. VILIP-1 down-regulation was obtained by transfecting cells with the siRNA duplex (referred to as V1-siRNA) using Lipofectamine 2000 according to the manufacturer's instructions. 100 pmol of siRNA complexed by 5 μ l of Lipofectamine 2000 was used in 1 ml of medium. Fluorescein-conjugated siRNA duplex was used for cotransfection with V1-siRNA or scrambled siRNA to identify cells incorporated with the siRNA duplex. The full-length cDNA of VILIP-1-EGFP was subcloned into a cytomegalovirus promoter-driven adenoviral vector (AdLox.HTM) via HindIII and XbaI, yielding Ad-VILIP-1-EGFP. The virus was created according to the protocol described previously (26). Recombinant adenovirus particles of Ad-VILIP-1-EGFP or the control virus (Ad-EGFP) produced after recombination were amplified by passage in CRE8 cells as described (26). Recombinant adenovirus particles (~10¹⁰ plaque-forming units/ml) were used to infect isolated mouse islets (multiplicity of infection of 10⁴, assuming 10³ β -cells/islet). Overexpression of VILIP-1 in MIN6 or single islet cells was achieved by transfection of VILIP-1-EGFP using Lipofectamine 2000 (27), and that in intact mouse islets by adenoviral transduction. A pilot study with the control virus Ad-EGFP demonstrated that 70–80% of the cells in islets were infected as detected by confocal fluorescence microscopy.

Evaluation of Insulin Secretion and Content in MIN6 Cells and Mouse Islets—MIN6 cells were seeded into 24-well plates and incubated for 48–72 h before glucose-stimulated insulin secretion (GSIS) studies. Cells were preincubated for 1 h in glucose-free Krebs-Ringer HEPES buffer (125 mM NaCl, 5.9 mM KCl, 1.28 mM CaCl₂, 5.0 mM NaCO₃, 25 mM HEPES, and 0.1% (w/v) bovine serum albumin) in a 37 °C humidified incubator. The cells were then incubated in the same buffer containing 2.8

TABLE 1

Primers for real-time PCR

PKB, protein kinase B; ERK, extracellular signal-regulated kinase; mTOR, mammalian target of rapamycin.

Gene name	Role	NCBI accession no.	Forward primer (5'–3')	Reverse primer (5'–3')
<i>akt1</i> /PKB	β -Cell proliferation	NM_009652	TGCATTGCCGAGTCCAGAA	CAGCGCATCCGAGAAACAA
<i>cdk4</i>	β -Cell proliferation	NM_009870	CTTTAACCACATAAAGCGAATCTCT	GCTTTCCTCCTTGTGCAGGTA
<i>c-myc</i>	MAPK/ERK growth and differentiation	NM_010849	CGGTTCCCTTCTGACAGAACTGA	CAGCCAAGGTTGTGAGGTTAGG
CREB	MAPK/ERK growth and differentiation	NM_009952	GCAGCAAGAGAATGTCGTAGAAAG	CCTCAATCAATGTTTTGTTTTGGT
Cyclin A ₂	DNA replication	NM_009828	CCTTGCAGCTCTGAAAATTTGTAAA	AGAGCATCCTGGCCTACATGTC
Cyclin D ₁	β -Cell proliferation	NM_007631	AGGCTACAGAAGAGTATTTATGGGAAAAG	TGCGTTTGAATCAAGGGAGAT
Cyclin D ₂	β -Cell proliferation	NM_009829	GTGAATTTGGGCTTCTACTTCCA	AGCGAATTCCTCCATCAGA
<i>foxo1</i>	β -Cell proliferation	NM_019739	GCGCATAGCACCAGTCTTCA	AGCGTGACACAGGGCATCA
Glucokinase	Glucose sensing	NM_028121	AGGCCCCACAGCTTGTCT	CAAAAGGAACGAGTAGCAGTCTTGT
<i>glut2</i>	Glucose sensing	NM_031197	CACATTCAAACGACTTCTGTACCT	TGTACGAAAACCCGAAGTCT
<i>gsk3b</i>	Survival	NM_019827	TCTGCTAAGGTGAGCTGATGACTAG	AACCACCTGGAGGGCAAGA
<i>ingap</i>	Islet neogenesis	NM_013893	GACAAAGGAGCGAGCATGATG	CAGCAGAGATGAGATGAGGAATTC
<i>irs2</i>	β -Cell proliferation	XM_357863	CATCGACTTCTGTCCATCA	CCCATCTCAAGGTCAAAGG
<i>mapk1</i>	MAPK/ERK growth and differentiation	NM_011949	CAGTTCCTTACCTGGTCTCT	CGCTCTGAAAGGCTCAAAGG
mTOR	β -Cell proliferation	NM_020009	CTAGAGCAGGTTGTGAGTTATAAGCAA	TTTACTCAGATACAACGTGGTGTCTAGA
<i>pdx-1</i>	β -Cell proliferation	NM_008814	CGGCTGAGCAAGCTAAGGTT	TGGAAGAAGCGCTCTCTTTGA
Insulin		NM_008386	ATCAGAGACCATCAGCAAGCAGGT	GGGACCACAAAGATGCTGTTTGC
β -Actin		NM_007393	AGATCTGGCACCACCTTCTACA	TTTCACGGTTGGCCTTAGGTTCA

mM (basal concentration) or 20 mM (stimulatory concentration) glucose for 1 h or 20 mM glucose with 20 mM arginine for 5 min. Islets (10/condition) were preincubated for two sequential 30-min periods in Krebs-Ringer HEPES buffer and for 2 h at the indicated glucose concentration (either 2.8 or 20 mM) (24). The supernatants of the cells were collected and centrifuged at 300 $g \times$ for 10 min to remove cell debris for insulin secretion assessment, and the cell pellets were lysed with acid ethanol (75% ethanol containing 1.5% (v/v) HCl) for DNA quantification or insulin content assessment (21). The insulin concentration in the supernatant or cell lysate was measured by radioimmunoassay as described previously (28). The insulin secretion data were normalized by total DNA content.

Measurement of Intracellular cAMP Content—Intracellular cAMP was measured as described previously (29). Briefly, the cells were washed with cold Krebs-Ringer HEPES buffer after removal of the supernatant. Intracellular cAMP was extracted with 80% ethanol and resuspended in cAMP assay buffer (0.05 mM sodium acetate (pH 6.2) and 0.01% sodium azide) and measured by radioimmunoassay using an intracellular cAMP assay kit.

Quantitative Real-time PCR—Total RNA was extracted from MIN6 cells using TRIzol reagent and further purified with RNeasy kits according to the manufacturer's instructions. Purified RNA was converted to cDNA using SuperScript II reverse transcriptase, and real-time PCR was performed using an ABI PRISM 7900HT sequence detection system (Applied Biosystems, Foster City, CA) according to the same protocol described previously (21). Primer Express Version 2.0 (Applied Biosystems) was used to design primers for real-time PCR. Platinum Taq DNA polymerase reagents were used to amplify target cDNA sequences, and SYBR Green was used to quantify PCR products. A standard curve was generated using mouse genomic DNA for quantification purposes. The measurements of gene expression were normalized by β -actin transcripts in the same sample. The sequences of the primers are shown in Table 1.

Luciferase Reporter Assay—24 h after siRNA duplex transfection, MIN6 cells were cotransfected with rat insulin I promoter-*Renilla* luciferase and cytomegalovirus promoter-*Renilla* luciferase (9:1 ratio); the latter was used for constitutive expression of *Renilla* luciferase as an internal control. 2 days after cotransfection, the cells were washed with cold phosphate-buffered saline and lysed with reporter buffer (Promega Corp.). The assay was performed using the Dual-Luciferase reporter assay system. The ratio of the activity of firefly to *Renilla* luciferase is presented as the relative luciferase activity. Luciferase expression without an upstream promoter was taken as the basal activity.

Fractionation, Immunoblotting, and Immunoprecipitation—Tissues and MIN6 cells were homogenized in lysis buffer (20 mM Tris-HCl (pH 7.5), 150 mM NaCl, 1 mM Na₂EDTA, 1 mM EGTA, 1% Triton, 2.5 mM sodium pyrophosphate, 1 mM β -glycerophosphate, 1 mM Na₃VO₄, 1 μ g/ml leupeptin, and 1 mM phenylmethylsulfonyl fluoride). The subcellular fractionation of MIN6 cells was performed according to the protocol of the Qproteome compartment kit. Differential speed centrifugation of the lysate was implemented to obtain subcellular fractions. The supernatant from the 1000 \times g centrifugation contained cytosolic proteins, that from the 6000 \times g centrifugation contained membrane proteins, and that from the 6800 \times g centrifugation contained nuclear proteins. The fractions or whole cell lysates were separated by 12% SDS-PAGE and transferred to polyvinylidene difluoride membranes. The rabbit polyclonal antibody against VILIP-1 used for immunoblotting has been described previously (30). The intensity of the appropriate immunoreactive bands was measured by densitometry, and the data were normalized by β -actin content as described (21) and analyzed using image analysis software (Scion Image Version 4.02, Scion Corp., Frederick, MD).

Immunoprecipitation was performed as described previously (31). Briefly, HEK293 cells transfected with the cDNA of VILIP-1, syntaxin-1, or SNAP25 were harvested in binding buffer (25 mM HEPES (pH 7.4), 100 mM KCl, 2 mM EDTA, 1%

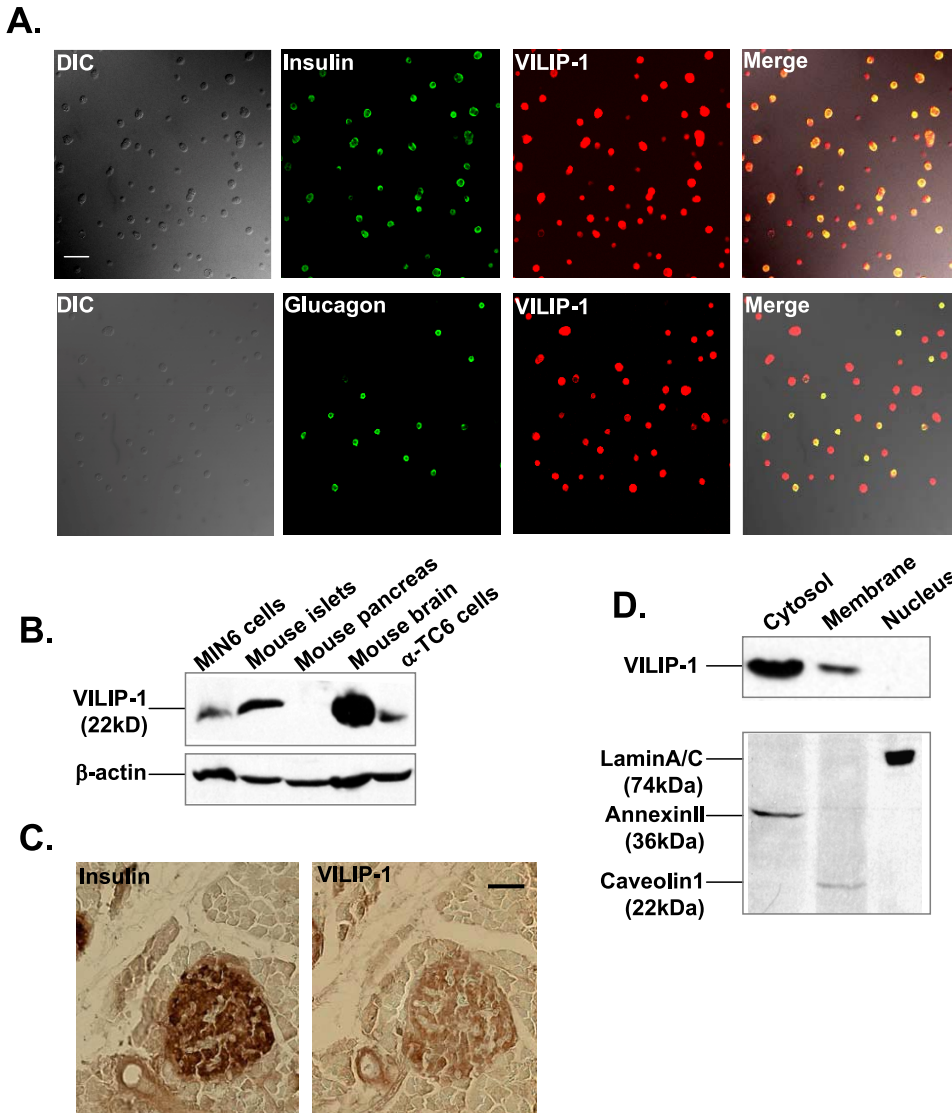


FIGURE 1. Expression of VILIP-1 in cells and tissues. *A*, immunostaining showing VILIP-1 expression in insulin-expressing cells (upper panels) and glucagon-expressing cells (lower panels). Scale bar = 50 μ m. DIC, differential interference contrast. *B*, Western blot showing VILIP-1 expression in MIN6 cells, isolated islets, mouse pancreatic extracts, mouse brain, and α -TC6 cells. *C*, immunohistochemistry of mouse pancreatic tissue showing VILIP-1 staining (right panel) and co-localization with insulin staining (left panel). Scale bar = 20 μ m. *D*, subcellular fractionation of MIN6 cell protein extracts showing VILIP-1 localization in cytosolic, membrane, and nuclear fractions (representative of three independent experiments).

Triton X-100, 20 μ M NaF, 1 mM phenylmethylsulfonyl fluoride, 2 μ M pepstatin A, 1 μ g/ml leupeptin, and 10 μ g/ml aprotinin). After sonification and centrifugation to remove cell debris, the supernatant was incubated overnight with glutathione *S*-transferase (GST; negative control), GST-syntaxin-1A, or GST-SNAP25 at 4 $^{\circ}$ C with constant agitation. Fusion proteins GST-syntaxin-1A and GST-SNAP25 were prepared as described (22, 23). All GST fusion proteins were bound to glutathione-agarose beads. The beads were washed three times with binding buffer. The eluants from the beads were separated by 12% SDS-PAGE; transferred to polyvinylidene difluoride membranes; and identified with rabbit anti-VILIP-1 polyclonal antibody (1:5000), mouse anti-syntaxin-1A monoclonal antibody (1:1000), or mouse anti-SNAP25 monoclonal antibody (1:1000).

The images were captured by confocal fluorescence microscopy.

Capacitance Measurements—Cells expressing EGFP or exhibiting fluorescein fluorescence were selected and patch-clamped in the whole cell configuration at 33 $^{\circ}$ C. The capacitance measurements were performed using an EPC-9 amplifier and PULSE software from HEKA Elektronik (Lambrecht, Germany). Patch pipettes were pulled from 1.5-mm thin-walled borosilicate glass tubes using a two-stage Narishige micropipette puller and had typical resistances of 3–6 megohms when fire polished and filled with an intracellular solution containing 120 mM CsCl, 20 mM tetraethylammonium chloride, 1 mM MgCl₂, 0.05 mM EGTA, 10 mM HEPES, 0.1 mM cAMP, and 5 mM MgATP, pH 7.3, with CsOH. Extracellular solutions contained 118 mM NaCl, 20 mM triethylammonium

Immunohistochemistry—Pancreases were fixed in 4% paraformaldehyde, dehydrated, and processed for paraffin embedding using routine procedures. Sections (5 μ m) were adhered to glass slides, rehydrated, and blocked with 3% H₂O₂ for 10 min. After being washed with phosphate-buffered saline, sections were incubated in appropriate non-immune serum (5%) for 30 min (goat for VILIP and rabbit for insulin). Sections were blotted to remove excess serum prior to overnight application of anti-insulin (1:1000) or anti-VILIP-1 (1:800) primary antibody (32) at 4 $^{\circ}$ C. Positive immunostaining was detected by incubating sections with goat anti-rabbit or rabbit anti-guinea pig peroxidase (1:100) for VILIP-1 and insulin, respectively, for 60 min at room temperature, followed by application of diaminobenzidine/H₂O₂ for 8 min.

Dispersed mouse islet cells on glass coverslips were fixed in 3.7% formaldehyde and permeabilized with 0.1% Triton X-100. After being washed with phosphate-buffered saline, the coverslips were blocked in 5% bovine serum albumin for 2 h before overnight application of primary antibody against VILIP-1, insulin, or glucagon at 4 $^{\circ}$ C. Cy5-conjugated donkey anti-rabbit secondary antibody was used to detect VILIP-1; fluorescein isothiocyanate (FITC)-conjugated rat anti-mouse and FITC donkey anti-guinea pig secondary antibodies were used to detect glucagon and insulin, respectively.

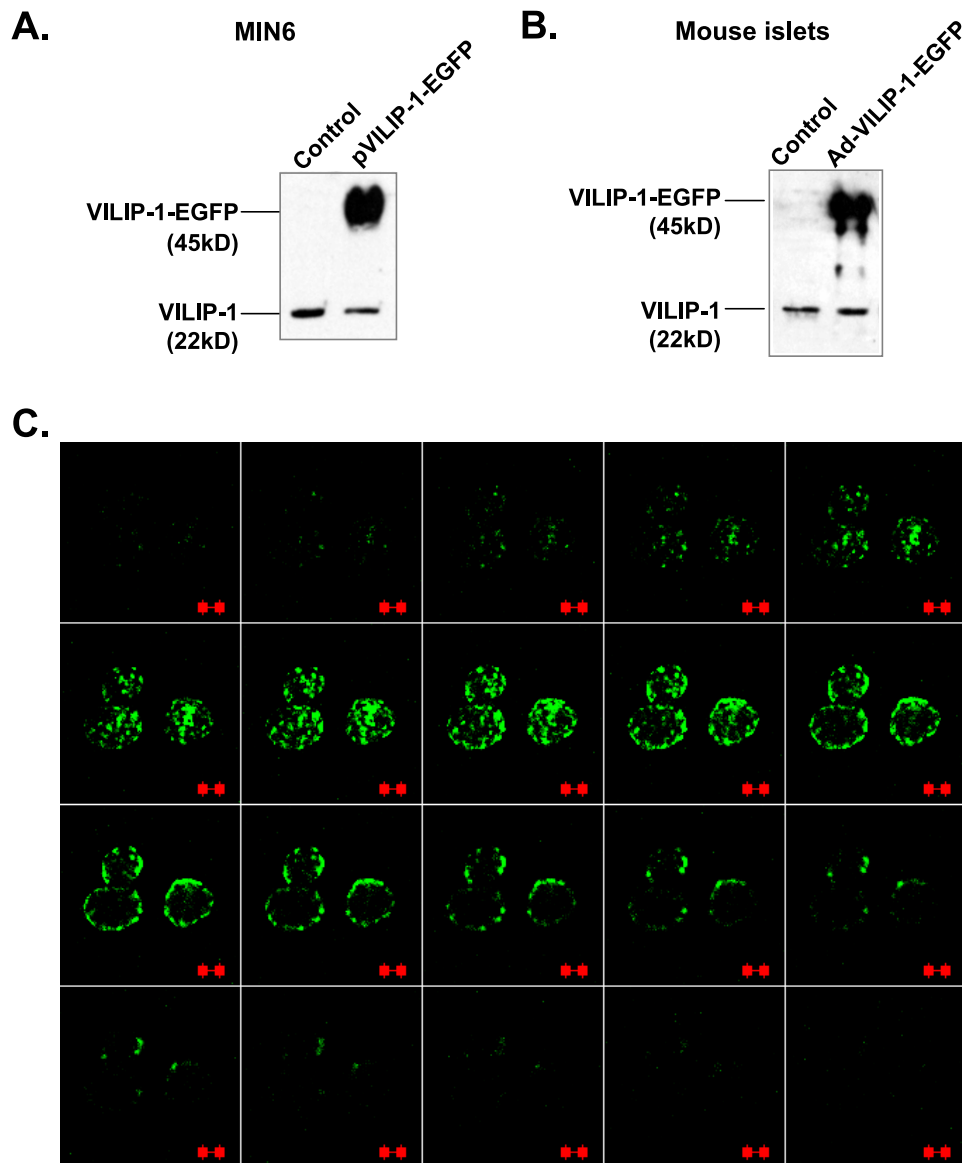


FIGURE 2. Assessment of VILIP-1 overexpression. *A* and *B*, overexpression of VILIP-1 in MIN6 cells via transfection with pVILIP-1-EGFP and in isolated mouse islets via adenoviral infection with Ad-VILIP-1-EGFP, respectively. The Western blots show VILIP-1-EGFP (45 kDa) overexpression in MIN6 cells (*A*) and in isolated mouse islets (*B*) as well as endogenous expression of VILIP-1 (22 kDa). *C*, confocal images of intact mouse islets showing the infection efficiency of Ad-VILIP-1-EGFP. Stack images were taken every 12.8 μm . Scale bar = 50 μm .

chloride, 2.6 mM CaCl_2 , 5 mM HEPES, 5.6 mM KCl, 1.2 mM MgCl_2 , and 20 mM glucose, pH 7.4, with NaOH.

Confocal Fluorescence Microscopy—Islets overexpressing VILIP-1-EGFP were analyzed using a Zeiss LSM-510 laser scanning confocal imaging system with a $\times 40$ water immersion Plan Apochromat objective. Samples were subjected to optical sectioning by moving the focal plane along the vertical (z) axis. HEK293 cells transiently transfected with VILIP-1-EGFP were treated with 1 mM ionomycin in Krebs-Ringer HEPES buffer. Serial images of these cells were taken every 15 s with the same apparatus.

Statistics—All data are presented as the means \pm S.E. Statistical comparisons were performed using Student's t test. Patch clamp data were analyzed with IGOR Pro Version 3.12 software

(WaveMetrics, Lake Oswego, OR). Differences were considered to be significant when $p < 0.05$.

RESULTS

Expression of VILIP-1 in Cells and Tissues—Immunostaining of dispersed mouse islets showed that VILIP-1 localized to insulin-expressing β -cells and glucagon-expressing α -cells (Fig. 1A). Western blotting showed VILIP-1 expression (~ 22 kDa) in MIN6 β -cells, α -TC6 cells, and intact isolated mouse islets (Fig. 1B). VILIP-1 was also highly expressed in mouse brain but was not detected in mouse pancreatic extracts, suggesting little or no expression in acinar tissue (Fig. 1B). Immunohistochemical analysis of serial mouse pancreatic sections showed that VILIP-1 immunoreactivity was confined to islets and overlapped with insulin, further confirming VILIP-1 deficiency in acinar tissue (Fig. 1C). Immunoblot analysis of subcellular compartment fractionation in MIN6 cells revealed that VILIP-1 could be detected in cytosolic and membrane fractions but not in the nuclear fraction using annexin II, caveolin-1, and lamin A/C as the marker proteins for the cytosolic, membrane, and nuclear fractions, respectively (Fig. 1D).

Assessment of VILIP-1 Overexpression in MIN6 Cells and Isolated Mouse Islets—Overexpression of VILIP-1 in MIN6 cells and single islet cells was accomplished by transient transfection of the pEGFP-N1 vector expressing a fusion protein, yielding pVILIP-1-EGFP, in which EGFP was fused to the C terminus of VILIP-1 (12). Based on EGFP fluorescence, the transfection efficiencies routinely ranged from 80 to 90% in MIN6 cells and from 5 to 10% in single islet cells (data not shown). To accomplish VILIP-1 overexpression in mouse intact islets, an adenovirus harboring the VILIP-1-EGFP cDNA was constructed (Ad-VILIP-1-EGFP). Western blot analysis confirmed overexpression of VILIP-1-EGFP in MIN6 cells and mouse intact islets (Fig. 2, *A* and *B*) using cells overexpressing EGFP driven by the same promoter as the control. A transduction efficiency of 70–80% with Ad-VILIP-1-EGFP was routinely achieved 48 h post-infection as observed by confocal fluorescence microscopy (Fig. 2C). All of the experiments were performed 48 h after plasmid transfection or viral infection.

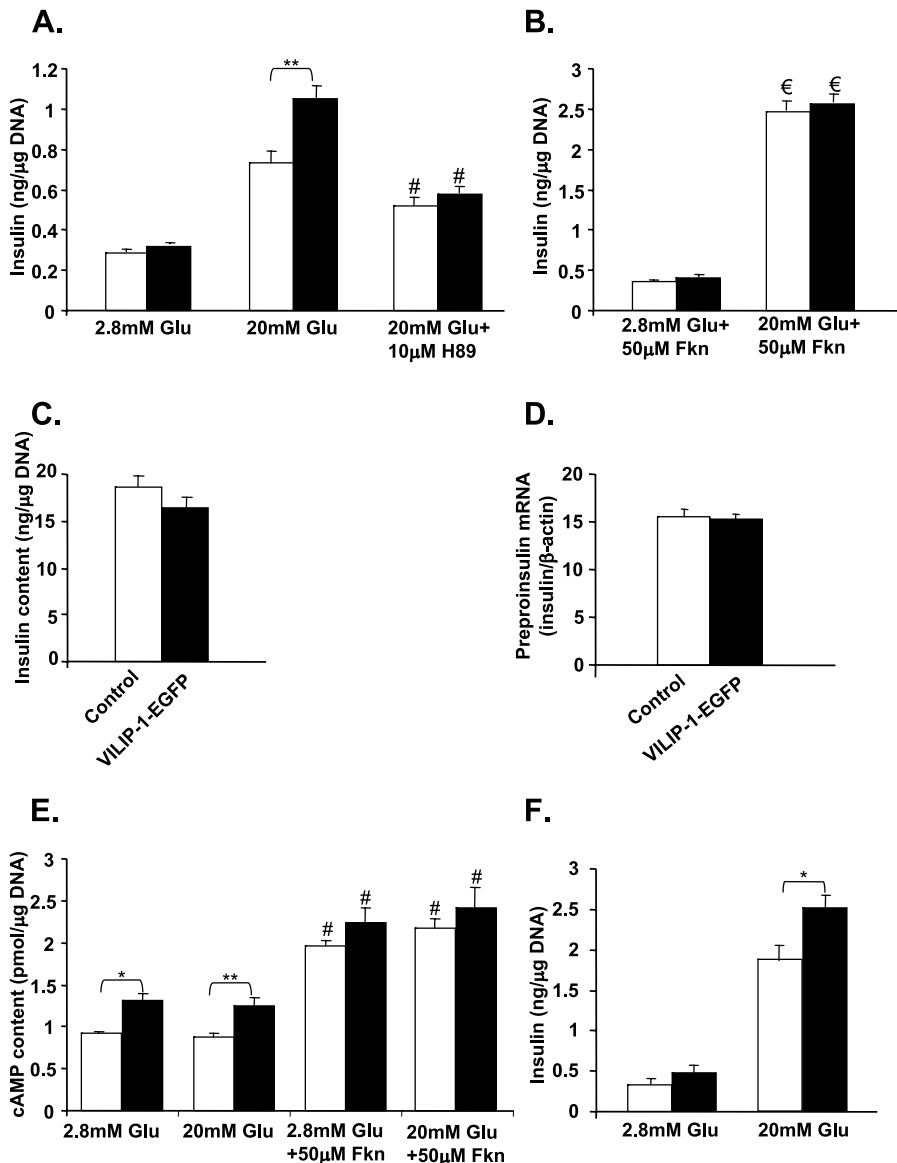


FIGURE 3. Effect of VILIP-1 overexpression on pancreatic β -cells. GSIS (A and B), insulin content (C), preproinsulin mRNA (D), and intracellular cAMP accumulation (E) in MIN6 cells were measured 48 h post-transfection with VILIP-1-EGFP. Insulin secretion in isolated mouse islets was evaluated 48 h post-viral infection (F). White bars, cells transfected with control EGFP; black bars, cells transfected with VILIP-1-EGFP. Data are the means \pm S.E. from three independent experiments carried out in three to four replicates. *, $p < 0.05$, and **, $p < 0.001$ compared with the control ($n \geq 9$); #, $p < 0.05$ compared with the counterpart without H-89 or forskolin (Fkn) treatment ($n \geq 9$); €, $p < 0.05$ compared with the corresponding value at 2.8 mM glucose ($n = 10$).

Effect of VILIP-1 Overexpression on GSIS, Insulin Content, and cAMP Content—Overexpression of VILIP-1 in MIN6 cells resulted in no significant effects on basal insulin secretion (Fig. 3A). However, a significant increase ($43 \pm 6.0\%$, $n = 12$; $p < 0.001$) in insulin secretion at 20 mM glucose compared with control cells was observed (1.05 ± 0.06 versus 0.73 ± 0.05 ng/ μ g of DNA, respectively) (Fig. 3A). This effect was also demonstrated in isolated mouse islets; overexpression of VILIP-1 with Ad-VILIP-1-EGFP had no effect on basal secretion but led to a $35 \pm 8.5\%$ increase ($n = 9$; $p < 0.05$) in GSIS (2.52 ± 0.16 versus 1.87 ± 0.18 ng/ μ g of DNA) (Fig. 3F). Forskolin, which increases cAMP by activating adenylyl cyclase, increased GSIS in control cells from 0.73 ± 0.05 to 2.46 ± 0.12 ng/ μ g of DNA ($n = 10$; $p <$

0.05) but had no significant effect on insulin secretion at the basal glucose concentration (Fig. 3, A and B). A similar phenomenon was observed in VILIP-1-overexpressing cells treated with forskolin; GSIS was increased from 1.05 ± 0.06 to 2.56 ± 0.09 ng/ μ g of DNA ($n = 10$; $p < 0.05$), with no change in insulin secretion at the basal glucose concentration (Fig. 3, A and B). Conversely, when VILIP-1-overexpressing MIN6 cells were treated with the protein kinase A (PKA) inhibitor H-89, insulin secretion dropped significantly by $45 \pm 8.0\%$ ($n = 12$; $p < 0.05$) from 1.05 ± 0.06 to 0.58 ± 0.06 ng/ μ g of DNA and was not significantly different from control cells (0.52 ± 0.03 ng/ μ g of DNA, $n = 12$; $p > 0.05$) (Fig. 3A). Furthermore, despite increased GSIS, total insulin content and preproinsulin mRNA in VILIP-1-overexpressing MIN6 cells remained unchanged (Fig. 3, C and D). Therefore, our results demonstrated that, although VILIP-1 overexpression had no effect on basal insulin secretion or preproinsulin mRNA, it could modestly enhance GSIS in a PKA-associated manner.

Previous studies have shown that VILIP-1 overexpression leads to increased cAMP accumulation (15). It is well known that cAMP can potentiate GSIS via PKA-dependent and PKA-independent pathways (33, 34). To establish a possible link between cAMP and increased GSIS in pancreatic β -cells overexpressing VILIP-1, we measured cAMP content in MIN6 cells. At 2.8 mM glucose, the cAMP content in the cells overexpressing VILIP-1 was increased by $43.5 \pm 3.8\%$ (1.32 ± 0.07 versus 0.91 ± 0.02 pmol/ μ g of DNA, $n = 9$; $p < 0.05$), whereas at 20 mM glucose, a $41.3 \pm 6.7\%$ increase ($n = 9$; $p < 0.001$) was observed (1.24 ± 0.09 versus 0.87 ± 0.05 pmol/ μ g of DNA) (Fig. 3E). The cAMP content was almost 2-fold higher in VILIP-1-overexpressing MIN6 cells treated with forskolin than in non-treated cells both at the basal glucose concentration (2.24 ± 0.16 versus 1.32 ± 0.07 pmol/ μ g of DNA, $n = 9$; $p < 0.05$) and at the stimulatory glucose concentration (2.41 ± 0.24 versus 1.24 ± 0.09 pmol/ μ g of DNA) (Fig. 3E). The cAMP content was also increased by 2-fold in control cells with forskolin treatment (1.96 ± 0.06 versus 0.91 ± 0.02 pmol/ μ g of DNA at the basal glucose concentration and 2.17 ± 0.11 versus

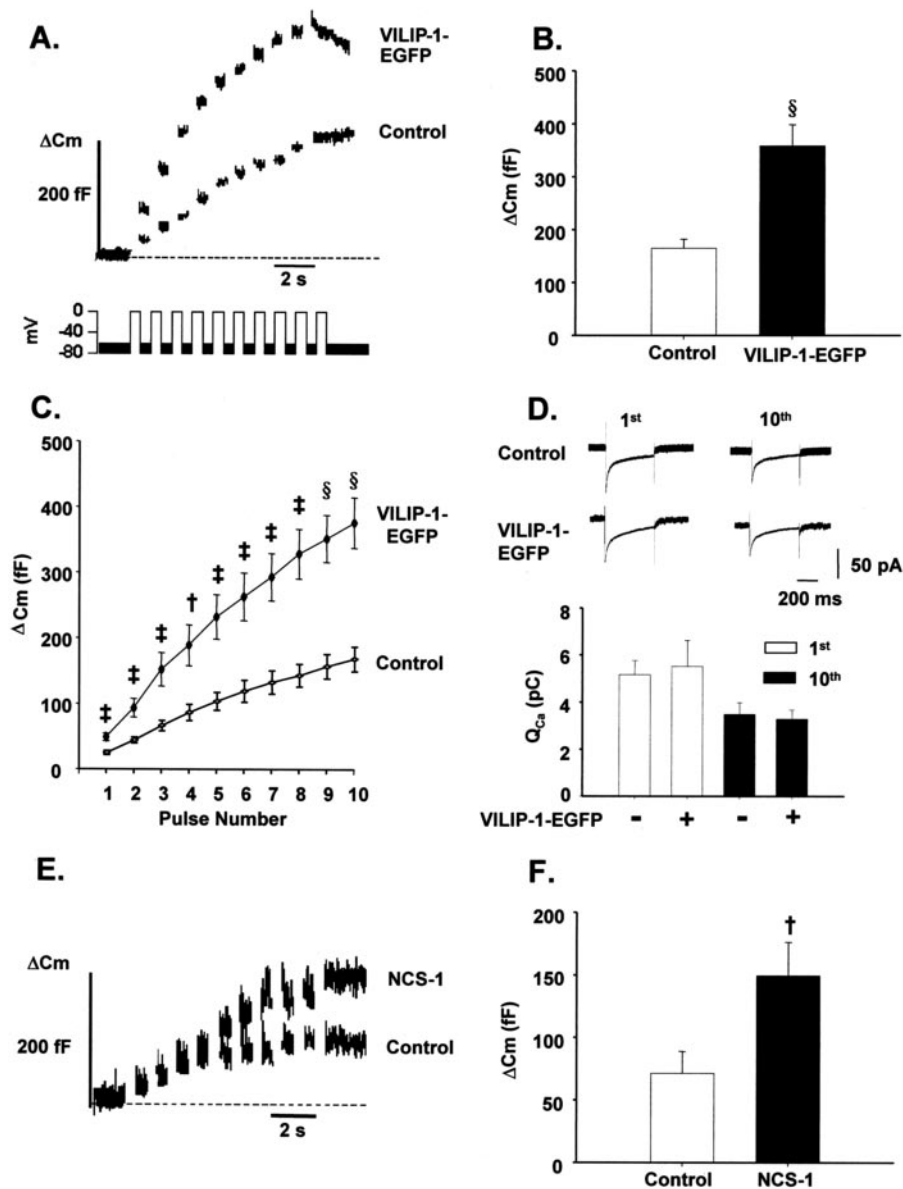


FIGURE 4. VILIP-1 overexpression enhances exocytosis in mouse β -cells. A train of ten 500-ms depolarizations from -70 to 0 mV was applied to mouse β -cells transfected with pEGFP (*Control*) or pVILIP-1-EGFP. Changes in cell membrane capacitance (ΔC_m) were measured at 20 mM glucose 2 days after transfection. *A*, representative ΔC_m traces recorded from a control β -cell (pEGFP) and a VILIP-1-EGFP-overexpressing β -cell. The electrical depolarization protocol is indicated below the corresponding traces. *B*, total increase in ΔC_m evoked by a train of depolarizations in cells overexpressing VILIP-1 and control EGFP ($n = 6$). *C*, summary data of cumulative increases in cell capacitance for each depolarizing pulse. *pC*, picocoulomb. *D*, representative Ca^{2+} currents and summary of integrated Ca^{2+} currents (Q_{Ca}) evoked by the first and tenth pulse during a train of 10 depolarizations. Currents were recorded associated with the capacitance measurements. *E* and *F*, representative traces and summary of ΔC_m , respectively, in cells transfected with EGFP (*Control*; $n = 8$) or NCS-1 ($n = 11$) used as a positive control for the effect of VILIP-1 on exocytosis according to Gromada *et al.* (27). Data are presented as the means \pm S.E. †, $p < 0.05$; ‡, $p < 0.01$; §, $p < 0.001$.

0.87 ± 0.05 pmol/ μ g of DNA at the stimulatory glucose concentration, $n = 9$; $p < 0.05$) (Fig. 3E).

Measurement of Cell Capacitance in Single β -Cells Overexpressing VILIP-1—cAMP can potentiate insulin secretion by various means, including acting directly on exocytosis (35). In pancreatic β -cells, exocytosis is regulated at several levels both temporally and spatially (36). The insulin granule pool consists of a low percentage of readily releasable pool (RRP) immediately accessible for release triggering and the reserve pool (RP)

that requires mobilization to RRP before docking (37). It was shown very recently by cell capacitance measurements that overexpression of NCS-1, a member of NCS family Group II, facilitates glucose-dependent exocytosis by increasing RRP via stimulation of phosphatidylinositol 4-kinase- β in pancreatic β -cells (Fig. 4, *E* and *F*) (27). Given these data, we performed cell capacitance measurements on single mouse β -cells to verify that VILIP-1 potentiates insulin secretion by directly stimulating exocytosis. At 20 mM glucose, the total increase in cell capacitance in control cells was 172 ± 19 femtofarads (fF) (Fig. 4, *A* and *B*) in response to a train of 10 depolarizations. Under the same conditions, cells overexpressing VILIP-1 demonstrated a much stronger exocytotic response evoked by the same depolarization (376 ± 38 fF) (Fig. 4, *A* and *B*). Compared with control cells, VILIP-1 overexpression augmented cell capacitance by 2.2 ± 0.3 -fold ($n = 6$; $p < 0.001$) (Fig. 4*B*). In general, exocytosis during the first two or three depolarizations is believed to represent the capacity of RRP, whereas exocytosis evoked by the subsequent depolarizations demonstrates the refilling of the RRP by mobilization of new granules from the RP (38, 39). Close inspection of the exocytotic events in this study revealed that the capacitance increase elicited by the first three depolarizations in the cells transfected with VILIP-1 was 152 ± 26 fF, markedly larger than that in control cells (69 ± 8 fF, $n = 6$; $p < 0.01$) (Fig. 4*C*). In addition, a consistent increase in cell capacitance was observed in response to the following seven additional depolarizations from 103 ± 13 fF in control cells to 224 ± 27 fF in VILIP-1-over-

expressing cells ($n = 6$; $p < 0.01$) (Fig. 4*C*), showing a more profound enhancement of the RRP refilling in VILIP-1-overexpressing cells. These results suggested that VILIP-1 overexpression in the pancreatic β -cells stimulated exocytosis by increasing RRP size and enhancing the refilling process of RRP through promoting granule priming from RP to RRP. It was noteworthy that, during the train of depolarizations, the Ca^{2+} currents in both VILIP-1-overexpressing and control cells declined because of inactivation, and there was no significant difference

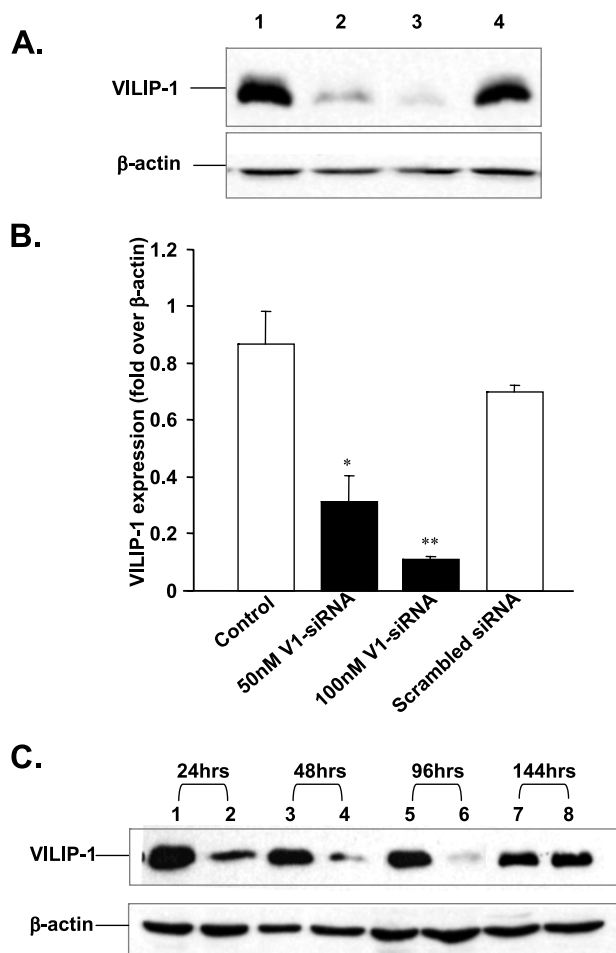


FIGURE 5. Down-regulation of VILIP-1 expression by V1-siRNA in MIN6 cells. *A*, Western blot showing VILIP-1 expression in MIN6 cells transfected with 50 nM (lane 2) or 100 nM (lane 3) siRNA duplex targeting VILIP-1 (V1-siRNA) or 100 nM scrambled siRNA (lane 4) 72 h post-transfection. Endogenous expression of VILIP-1 in untransfected MIN6 cells is shown in lane 1. *B*, expression of VILIP-1 as shown in *A* quantified by densitometry. Relative expression levels are reported as -fold change in VILIP-1 over β -actin. The means \pm S.E. are from three independent experiments. * and **, $p < 0.05$ and $p < 0.001$, respectively, compared with controls. *C*, time course of VILIP-1 expression in MIN6 cells transfected with V1-siRNA (lanes 2, 4, 6, and 8) or scrambled siRNA (lanes 1, 3, 5, and 7). Expression of VILIP-1 was measured 24 h (lanes 1 and 2), 48 h (lanes 3 and 4), 96 h (lanes 5 and 6), or 144 h (lanes 7 and 8) post-transfection. The blot is representative of three independent experiments.

in the integrated Ca^{2+} current between these two cells (Fig. 4D). This indicated that the effect of VILIP-1 on exocytosis was not caused by an increase in Ca^{2+} influx.

Assessment of MIN6 Cells Transfected by the siRNA Duplex against VILIP-1—To further investigate the role of VILIP-1 in the pancreatic β -cell, we reduced VILIP-1 expression in the MIN6 β -cells by transiently transfecting MIN6 cells with siRNA duplexes against VILIP-1 mRNA (V1-siRNA). The control siRNA duplex was previously shown not to have any observable effects in MIN6 cells (25) and in the present study had no effect on a variety of parameters, including VILIP-1 and β -actin expression (Fig. 5A), insulin secretion, and cAMP production (data not shown), compared with non-transfected MIN6 cells. At 72 h post-transfection with V1-siRNA, expression of VILIP-1 was decreased by $55 \pm 14\%$ ($p < 0.05$) compared with the control using 50 nM siRNA and

by $85 \pm 2\%$ ($p < 0.05$) using 100 nM siRNA (Fig. 5B). The suppression of VILIP-1 protein was observed for at least ~ 96 h post-transfection, with endogenous levels returning to the control level within 144 h (Fig. 5C). The VILIP-1 and control siRNA duplexes described above were used in all subsequent studies, with experiments being performed 72 h post-transfection (100 nM siRNA was used).

Effect of VILIP-1 Down-regulation on Insulin Secretion, Insulin Content, and cAMP Content in MIN6 Cells—To examine the consequences of significantly reducing VILIP-1 expression in MIN6 cells, insulin secretion assays were performed. Interestingly, compared with control cells, down-regulation of VILIP-1 resulted in a significant increase (2.14 ± 0.29 , $n = 21$; $p < 0.001$) in basal insulin secretion (0.51 ± 0.05 versus 0.23 ± 0.02 ng/ μ g of DNA, respectively) (Fig. 6A). In the presence of a stimulatory glucose concentration (20 mM), the insulin secretion was higher in cells expressing V1-siRNA than in those expressing control siRNA (0.91 ± 0.06 versus 0.61 ± 0.03 ng/ μ g of DNA, respectively, $n = 20$; $p < 0.001$) (Fig. 6A). When treated with H-89, MIN6 cells expressing V1-siRNA demonstrated decreased GSIS compared with those without treatment (from 0.91 ± 0.06 to 0.57 ± 0.11 ng/ μ g of DNA, $n = 9$; $p < 0.001$). However, GSIS in V1-siRNA cells with H-89 treatment was still larger than that in control cells (0.57 ± 0.11 versus 0.41 ± 0.04 ng/ μ g of DNA, $n = 9$; $p < 0.05$) (Fig. 6A). Despite enhanced insulin secretion, the cAMP content in MIN6 cells transfected with V1-siRNA was significantly decreased by $26.3 \pm 4.1\%$ ($n = 15$; $p < 0.001$) compared with control cells at the basal glucose concentration (0.73 ± 0.02 versus 0.99 ± 0.04 pmol/ μ g of DNA) and by $27.1 \pm 6.5\%$ ($n = 12$; $p < 0.05$) at 20 mM glucose (0.63 ± 0.04 versus 0.87 ± 0.06 pmol/ μ g of DNA) (Fig. 6B). H-89 treatment had no effect on cAMP accumulation in either V1-siRNA-expressing cells or control cells because PKA is downstream of cAMP (Fig. 6B). Thus, the augmented insulin secretion was attributed to mechanisms other than altered cAMP accumulation. To examine the capacity of MIN6 cells to secrete insulin, 20 mM arginine in the presence of glucose stimulus was used and shown to increase secretion significantly in V1-siRNA cells compared with control cells (1.41 ± 0.08 versus 1.00 ± 0.09 ng/ μ g of DNA, $n = 10$; $p < 0.001$) (Fig. 6A). This increased insulin capacity was supported by total insulin content measurement in V1-siRNA-transfected MIN6 cells, which was increased ($66 \pm 0.05\%$, $n = 15$; $p < 0.001$) compared with control cells (42.8 ± 1.2 versus 25.8 ± 0.8 ng/ μ g of DNA) (Fig. 6C). H-89 did not abolish this effect (33.3 ± 2.3 ng/ μ g of DNA in V1-siRNA cells versus 19.4 ± 1.8 ng/ μ g of DNA in control cells, $n = 9$; $p < 0.05$), although H-89 did decrease insulin content in both groups (Fig. 6C). To examine insulin expression in V1-siRNA-transfected MIN6 cells, we performed real-time PCR on RNA from these cells. Our results showed that preproinsulin mRNA in V1-siRNA cells was significantly increased by $54 \pm 14.7\%$ ($n = 12$; $p < 0.001$) over that in control cells (Fig. 6D). These results suggested that down-regulation of VILIP-1 likely induced insulin gene transcription independent of the cAMP/PKA pathway. To further verify induction of insulin gene transcription, we performed luciferase assays in which luciferase expression was driven by the rat insulin I promoter. The relative activity of luciferase

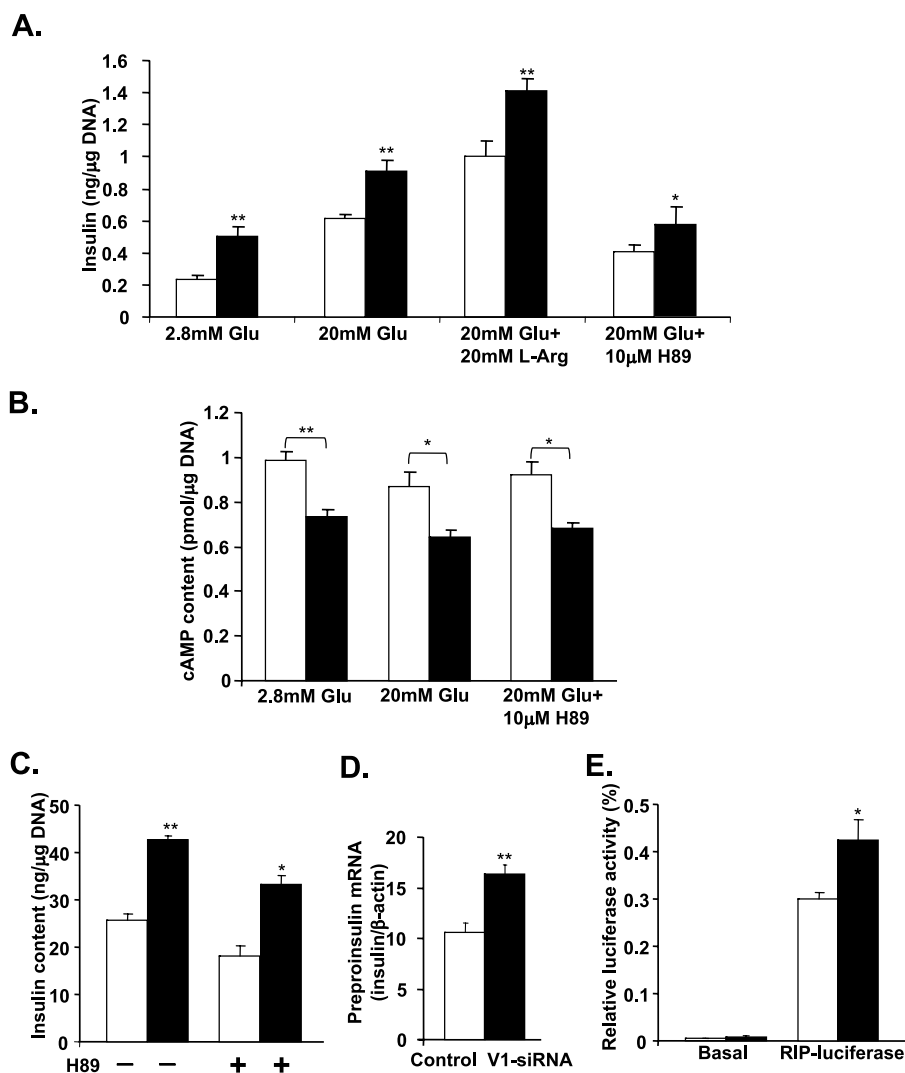


FIGURE 6. Effect of VILIP-1 down-regulation on MIN6 cell function. Insulin secretion (A), cAMP accumulation (B), insulin content (C), preproinsulin mRNA (D), and luciferase expression (E) in MIN6 cells were measured 72 h post-transfection with V1-siRNA (black bars) or control siRNA (white bars). The value of preproinsulin mRNA obtained by real-time PCR was normalized by β -actin transcripts in the sample. Expression of luciferase is presented as the ratio of the activity of rat insulin I promoter-driven firefly luciferase (RIP-luciferase) to that of the constitutively expressed *Renilla* luciferase. Luciferase expression without an upstream promoter was taken as the basal condition. Results are the means \pm S.E. from three independent experiments carried out in three to four replicates. * and **, $p < 0.05$ and $p < 0.001$ ($n \geq 9$), respectively, compared with the control.

ase in V1-siRNA-expressing cells was significantly increased ($41 \pm 3\%$, $n = 9$; $p < 0.05$) compared with that in control cells (Fig. 6E).

Effect of VILIP-1 Down-regulation on Cell Capacitance—Cell capacitance measurements record changes in the size of the insulin granule pool in single cells. To verify that VILIP-1 down-regulation caused an increase in total insulin content, we measured cell capacitance in MIN6 cells expressing V1-siRNA. MIN6 cells were cotransfected with V1-siRNA or control siRNA and fluorescein-conjugated scrambled siRNA (4:1 ratio). The fluorescein-conjugated siRNA served as a nonsense siRNA for optimal negative control and demonstrated siRNA incorporation into cells. Single cells demonstrating fluorescein were selected for cell capacitance measurements. Throughout the depolarization, the increase in cell capacitance in MIN6 cells expressing V1-siRNA was almost 2-fold of that in control cells (201 ± 35 versus 112 ± 20 fF, $n = 7$; $p < 0.05$) (Fig. 7). This

finding suggested that the size of the insulin granule pool was increased in V1-siRNA-expressing cells, further confirming the previous finding that VILIP-1 knockdown caused an enlarged insulin secretion capacity.

Gene Expression in MIN6 Cells with VILIP-1 Overexpression or Down-regulation—Our results indicated that VILIP-1 can play different roles in pancreatic β -cells depending on its expression level. To further investigate the genes regulated by VILIP-1 expression, we performed quantitative real-time PCR on total RNA extracted from MIN6 cells after VILIP-1 overexpression or down-regulation. Of 16 genes involved in β -cell replication, proliferation, and glucose sensing, we found that expression of cAMP-responsive element-binding protein (CREB), cyclin D₂, *Gsk3b*, and the pancreatic homeodomain transcription factor *pdx-1* was affected (Fig. 8, A and B). Expression of CREB, a downstream target of cAMP and PKA (40), was $128 \pm 36\%$ higher in MIN6 cells overexpressing VILIP-1 than in control cells (Fig. 8A). Conversely, CREB expression was decreased by $56 \pm 0.5\%$ in MIN6 cells with VILIP-1 down-regulation (Fig. 8B). Similarly, cyclin D₂, essential for postnatal β -cell growth (41), was up-regulated by $39 \pm 10\%$ in VILIP-1-overexpressing cells but down-regulated by $65 \pm 14\%$ in V1-siRNA-expressing cells. *Gsk3b*, a component of the

AKT/protein kinase B cell cycle regulation pathway (42), was induced by $62 \pm 29\%$ in VILIP-1-overexpressing cells (Fig. 8A). *pdx-1*, which directly regulates insulin transcription through formation of a complex with transcriptional coactivators on the proximal insulin promoter (43), was unchanged in MIN6 cells overexpressing VILIP-1 (Fig. 8A). However, in cells with VILIP-1 down-regulation, *pdx-1* expression was elevated up to $46 \pm 15\%$ (Fig. 8B).

DISCUSSION

The NCS family, a group of EF-hand-containing proteins, plays a variety of roles in cell signaling (44), including regulation of ion channel function (4), activation of multiple target proteins such as kinases (6), and interactions with nucleic acids and control of cyclic nucleotide levels (5, 19). In this study, we investigated VILIP-1 expression and its biological function in pancreatic β -cells. Our results showed that VILIP-1 was indeed

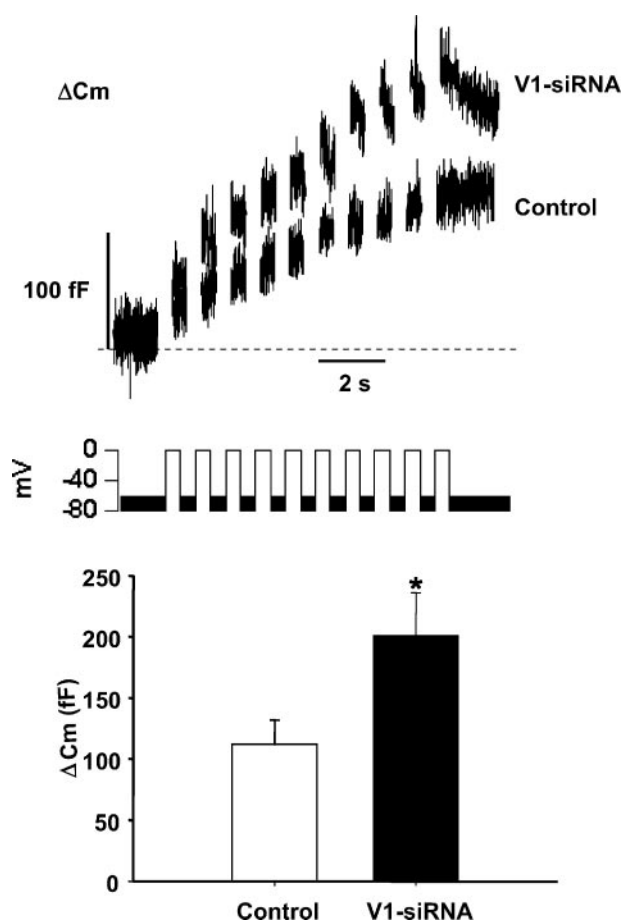


FIGURE 7. **VILIP-1 down-regulation enhances cell capacitance.** Shown are representative traces of ΔC_m recorded from MIN6 cells expressing V1-siRNA or control siRNA 72 h post-transfection (*upper panel*) and the total increase in ΔC_m evoked by a train of depolarizations in MIN6 cells expressing V1-siRNA or control siRNA ($n = 7$) (*lower panel*). The train of 500-ms depolarizations from -70 to 0 mV applied in the presence of 20 mM glucose is indicated below the traces. $^* p < 0.05$.

expressed in mouse pancreatic islets (β - and α -cells) but not in acinar tissue (Fig. 1). Although VILIP-1 could not be detected in the whole pancreas, islet cells, which occupy only a small fraction of the whole pancreas, showed strong VILIP-1 expression. Expression of VILIP-1 within the endocrine pancreas suggests a potential role in islet function.

It has been well demonstrated that VILIP-1 is involved in cAMP and cGMP signaling by modulating the cyclic nucleotide level in neurons (14, 15, 17, 30). Early studies showed that VILIP-1 overexpression in glioma cells enhances β -adrenergic receptor-stimulated cAMP accumulation and that this effect is still seen after stimulation of adenylyl cyclase with forskolin (15), indicating that VILIP-1 acts downstream of the receptor. Subsequent studies provided more evidence implicating the role of VILIP-1 in adenylyl cyclase modulation (11, 16). In a Ca^{2+} -dependent manner, VILIP-1 associates with membrane structures to interact with proteins, including adenylyl cyclase (11, 12, 45). In our study, in agreement with the findings in neurons, we found that VILIP-1 overexpression resulted in elevated cAMP accumulation in pancreatic β -cells (Fig. 3E). In contrast, VILIP-1 knockdown caused decreased cAMP levels (Fig. 6B). As shown in a previous study (11), VILIP-1-EGFP

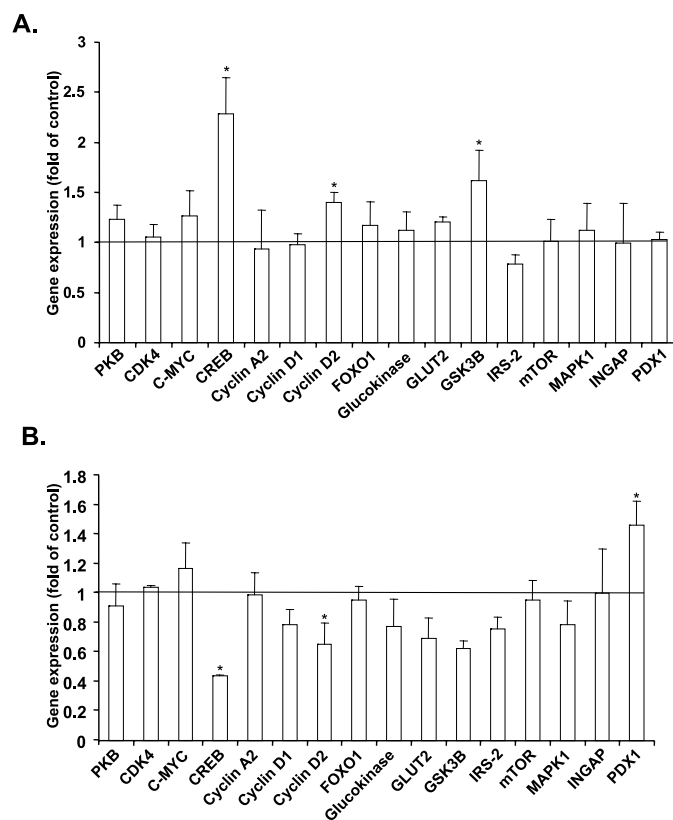


FIGURE 8. **Expression levels of selected genes in MIN6 cells.** Shown is the gene expression in MIN6 cells overexpressing VILIP-1-EGFP (A) and with VILIP-1 knockdown (B). Gene expression is expressed as -fold change over control cells. Data are presented as the means \pm S.E. from three independent experiments carried out in triplicate. $^* p < 0.05$ ($n = 9$).

expressed in HEK293 cells translocated from the cytosol to the plasma membrane (supplemental Fig. 1) upon stimulation with ionomycin (a Ca^{2+} ionophore). This translocation is considered to facilitate adenylyl cyclase modulation. Thus, cAMP may possibly be a downstream molecule through which Ca^{2+} and subsequently VILIP-1 exert their biological functions.

It is well known that cAMP, as a second messenger in the amplification pathway of stimulus coupling in β -cells, enhances insulin secretion only in the presence of stimulatory glucose concentrations. In MIN6 cells and mouse islets, VILIP-1 overexpression led to enhanced GSIS without significant effects on basal insulin secretion (Fig. 3, A and F). Enhanced GSIS can be mimicked by forskolin, which stimulates adenylyl cyclase to activate cAMP/PKA signaling cascades, leading to increased insulin secretion at stimulatory glucose concentrations (46). The increased GSIS observed in VILIP-1-overexpressing cells was blocked by the PKA inhibitor H-89, confirming that this effect is dependent upon the cAMP/PKA pathway. In our study, we used 2.8 mM glucose as the low glucose condition, which is likely insufficient for cAMP to potentiate insulin secretion. This could provide an explanation for our observation in VILIP-1-overexpressing β -cells that insulin secretion was enhanced at high but not basal glucose concentrations. Consistent with our findings, cAMP accumulation elicited by genistein, a soy isoflavone, stimulates insulin secretion in mouse islets at high but not low glucose concentrations (47).

cAMP can potentiate insulin secretion in several ways.

VILIP-1 and Insulin Secretion

These include increasing voltage-sensitive Ca^{2+} channel opening (48) and Ca^{2+} influx (49), activating ryanodine receptors in the endoplasmic reticulum (50), stimulating lipolysis (51), and directly acting on the exocytotic machinery (35). Most of these actions are mediated by the protein PKA pathway, but the direct effect on exocytosis is partly PKA-independent (34), being mediated by the cAMP-binding protein cAMP-regulated guanine nucleotide exchange factor II (53). In pancreatic β -cells, the insulin granule pool consists of a small RRP that is immediately accessible for release and a large RP that refills the RRP by granule mobilization (37). In general, a PKA-independent process increases the release probability of granules already in the RRP, whereas a PKA-dependent process promotes the refilling of the RRP by stimulation of mobilization of granules from the RP (34). VILIP-1 overexpression significantly increased exocytosis in response to the train of depolarizations in single β -cells compared with control cells (Fig. 4). This result is consistent with what has been observed with a related NCS protein, NCS-1. Gromada *et al.* (27) demonstrated that NCS-1 is expressed in pancreatic β -cells and that overexpression stimulates insulin exocytosis via phosphatidylinositol 4-kinase- β . Our results in VILIP-1-overexpressing cells employing capacitance recordings suggested that VILIP-1 increased the size and promoted the refilling of the RRP by stimulating the mobilization of granules in the RP, thereby increasing the capacity for exocytosis. It is known that NCS-1 partially co-localizes with the synaptic protein SNAP25 at the plasma membrane in NG108-15 cells (a mouse neuroblastoma and rat glioma hybrid) and that this interaction may facilitate exocytosis (54). However, in our study, immunoprecipitation experiments showed no interaction between VILIP-1 and the SNARE (soluble *N*-ethylmaleimide-sensitive factor attachment protein receptor) proteins syntaxin-1A and SNAP25 (supplemental Fig. 2) (31). Thus, our data suggested that VILIP-1 overexpression increased cAMP accumulation in pancreatic β -cells and potentiated insulin secretion via a cAMP-dependent effect on insulin exocytosis.

It is noteworthy that, in addition to stimulation of exocytosis in β -cells, activation of the cAMP/PKA pathway stimulates insulin gene transcription (55, 56). More recently, it has been shown that GLP-1, through activation of the cAMP/PKA pathway, increases the levels of PDX-1 protein and its translocation from the cytosol to nuclei in insulin-secreting RIN 1046-38 cells (57). PDX-1 is involved in several aspects of pancreatic β -cells function, including the positive regulation of insulin gene transcription (58), and directly activates insulin transcription by forming complexes with coactivators on the proximal insulin promoter (43). In our study, however, despite elevated cAMP accumulation, no change in either preproinsulin mRNA or *pdx-1* expression was observed with VILIP-1 overexpression. Conversely, in MIN6 cells transfected with V1-siRNA, despite decreased cAMP accumulation, insulin content and preproinsulin mRNA were actually increased. Therefore, insulin secretion at both basal and stimulatory glucose concentrations was elevated accordingly, whereas H-89 did not abolish this effect (Fig. 6). Of further interest, *pdx-1* gene expression was actually up-regulated, and insulin gene transcription was accordingly stimulated (Figs. 6

and 8). It appears that VILIP-1, via an alternative pathway, may exert inhibitory effects on insulin gene transcription, possibly through the suppression of *pdx-1*, and that this effect is independent of the cAMP/PKA pathway. These two pathways thus may allow dual effects of VILIP-1 in β -cells, stimulating insulin exocytosis and inhibiting insulin gene transcription. Although we have observed increased insulin gene transcription and content in VILIP-1 knockdown β -cells, we have not yet conclusively shown a direct effect on proinsulin biosynthesis.

Our data suggest that VILIP-1 may act in part as an insulin gene repressor, either directly or indirectly. Interestingly, VILIP-1 has been shown to bind to double-stranded RNA (19), implying a possible role of this protein in the regulation of gene expression. In addition, another NCS protein, KChIP3/DREAM (Kv channel-interacting protein-3/downstream regulatory element antagonistic modulator), a member of NCS protein family, has been reported to repress dynorphin gene transcription and production of dynorphin A peptides, which are involved in memory acquisition and pain. This effect is exerted directly on the prodynorphin promoter (5). Thus, previous studies and our present findings suggest a possible role of VILIP-1 in gene regulation. As for the mechanism, more studies are required to elucidate whether VILIP-1 itself acts as a transcription regulator or exerts its effect via other molecules to regulate genes like *pdx-1* and insulin.

VILIP-1 expression also influenced expression of genes involved in cell proliferation and cell cycle regulation (cyclin D_2 , *Gsk3b*, and CREB) (Fig. 8). Cyclin D_2 associates with the cyclin-dependent kinase CDK4 or CDK6 to promote cell cycle progression (59) and in rodents is required for postnatal islet growth and glucose homeostasis throughout life, as revealed by cyclin D_2 ($-/-$) mice (60). *Gsk3b* is linked with phosphorylation and proteolytic turnover of cyclin D_1 during the cell division cycle and thus has effects on cell cycle regulation (42). CREB is a direct downstream transactivator of the cAMP/PKA pathway, and stimulation of the cAMP pathway leads to PKA-mediated phosphorylation of CREB, which is found to occupy up to 4000 promoter sites *in vivo* and therefore can have profound effects on a variety of cellular processes (52). Further direct evidence is needed to demonstrate specific effects of VILIP-1 on cell proliferation and cell replication.

In summary, this is the first study demonstrating that VILIP-1, an NCS protein, is expressed in pancreatic α - and β -cells and is involved in the regulation of insulin secretion and insulin gene expression. Increased VILIP-1 enhanced GSIS in a cAMP-associated manner, whereas down-regulation of VILIP-1 was accompanied by decreased cAMP accumulation but increased insulin content. This study further supports a role for NCS proteins and in particular VILIP-1 in islet function.

REFERENCES

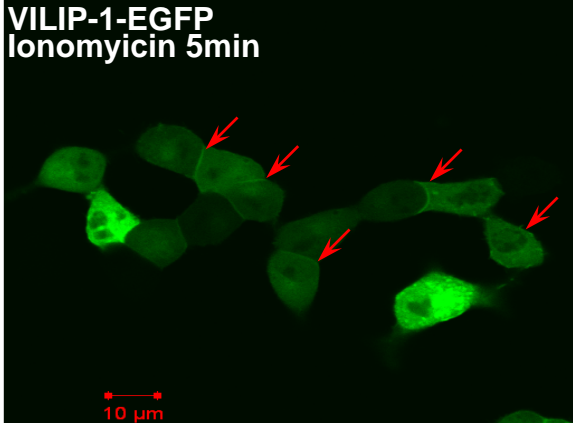
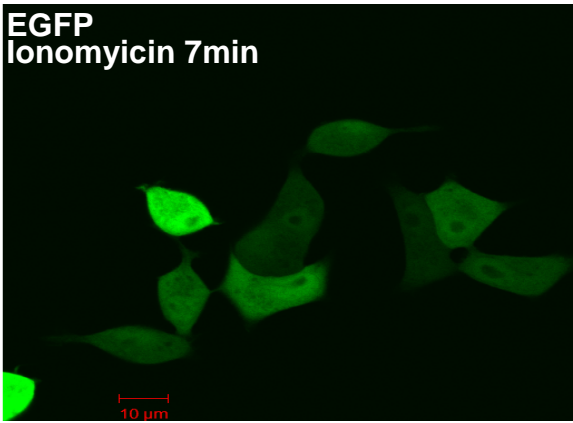
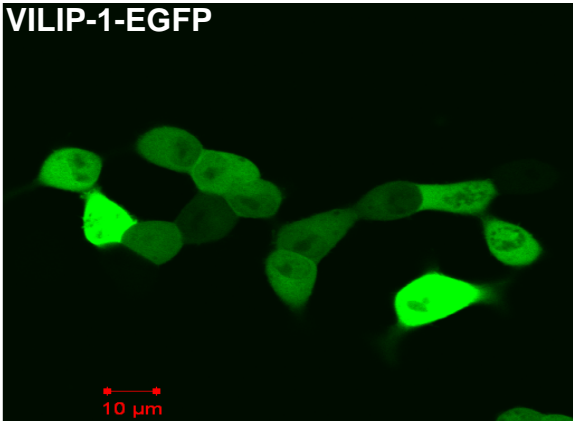
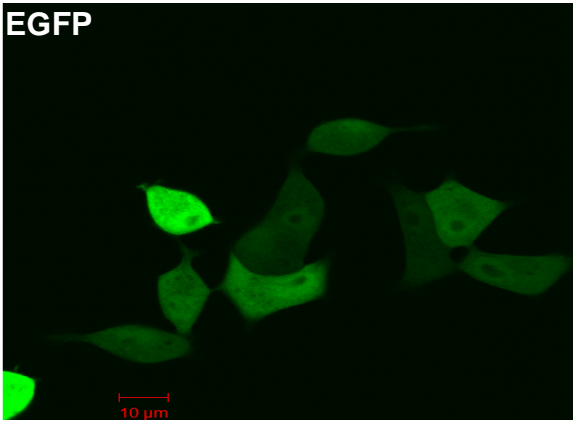
1. Brauneuwel, K.-H., and Gundelfinger, E. D. (1999) *Cell Tissue Res.* **295**, 1–12
2. Ames, J. B., Ishima, R., Tanaka, T., Gordon, J. I., Stryer, L., and Ikura, M. (1997) *Nature* **389**, 198–202
3. An, W. F., Bowlby, M. R., Betty, M., Cao, J., Ling, H. P., Mendoza, G., Hinson, J. W., Mattsson, K. I., Strassle, B. W., Trimmer, J. S., and Rhodes, K. J. (2000) *Nature* **403**, 553–556

4. Weiss, J. L., Archer, D. A., and Burgoyne, R. D. (2000) *J. Biol. Chem.* **275**, 40082–40087
5. Carrion, A. M., Link, W. A., Ledo, F., Mellstrom, B., and Naranjo, J. R. (1999) *Nature* **398**, 80–84
6. Hendricks, K. B., Wang, B. Q., Schnieders, E. A., and Thorner, J. (1999) *Nat. Cell Biol.* **1**, 234–241
7. Rajebhosale, M., Greenwood, S., Vidugiriene, J., Jeromin, A., and Hilfiker, S. (2003) *J. Biol. Chem.* **278**, 6075–6084
8. Zheng, Q., Bobich, J. A., Vidugiriene, J., McFadden, S. C., Thomas, F., Roder, J., and Jeromin, A. (2005) *J. Neurochem.* **92**, 442–451
9. Kuno, T., Kajimoto, Y., Hashimoto, T., Mukai, H., Shirai, Y., Saeki, S., and Tanaka, C. (1992) *Biochem. Biophys. Res. Commun.* **184**, 1219–1225
10. Polymeropoulos, M. H., Ide, S., Soares, M. B., and Lennon, G. G. (1995) *Genomics* **29**, 273–275
11. Lin, L., Braunewell, K.-H., Gundelfinger, E. D., and Anand, R. (2002) *Biochem. Biophys. Res. Commun.* **296**, 827–832
12. Spilker, C., Dresbach, T., and Braunewell, K.-H. (2002) *J. Neurosci.* **22**, 7331–7339
13. Lin, L., Jeanclos, E. M., Treuil, M., Braunewell, K.-H., Gundelfinger, E. D., and Anand, R. (2002) *J. Biol. Chem.* **277**, 41872–41878
14. Brackmann, M., Schuchmann, S., Anand, R., and Braunewell, K.-H. (2005) *J. Cell Sci.* **118**, 2495–2505
15. Braunewell, K.-H., Spilker, C., Behnisch, T., and Gundelfinger, E. D. (1997) *J. Neurochem.* **68**, 2129–2139
16. Mahloogi, H., Gonzalez-Guerrico, A. M., Lopez, D. C., Bassi, D. E., Goodrow, T., Braunewell, K.-H., and Klein-Szanto, A. J. (2003) *Cancer Res.* **63**, 4997–5004
17. Braunewell, K.-H., Brackmann, M., Schaupp, M., Spilker, C., Anand, R., and Gundelfinger, E. D. (2001) *J. Neurochem.* **78**, 1277–1286
18. Boekhoff, I., Braunewell, K.-H., Andreini, I., Breer, H., and Gundelfinger, E. (1997) *Eur. J. Cell Biol.* **72**, 151–158
19. Mathisen, P. M., Johnson, J. M., Kawczak, J. A., and Tuohy, V. K. (1999) *J. Biol. Chem.* **274**, 31571–31576
20. Gierke, P., Zhao, C., Brackmann, M., Linke, B., Heinemann, U., and Braunewell, K.-H. (2004) *Biochem. Biophys. Res. Commun.* **323**, 38–43
21. Wang, X., Li, H., De Leo, D., Guo, W., Koshkin, V., Fantus, I. G., Giacca, A., Chan, C. B., Der, S., and Wheeler, M. B. (2004) *Diabetes* **53**, 129–140
22. Kang, Y., Leung, Y. M., Manning-Fox, J. E., Xia, F., Xie, H., Sheu, L., Tsushima, R. G., Light, P. E., and Gaisano, H. Y. (2004) *J. Biol. Chem.* **279**, 47125–47131
23. MacDonald, P. E., Wang, G., Tsuk, S., Dodo, C., Kang, Y., Tang, L., Wheeler, M. B., Cattral, M. S., Lakey, J. R., Salapatek, A. M., Lotan, I., and Gaisano, H. Y. (2002) *Mol. Endocrinol.* **16**, 2452–2461
24. Joseph, J. W., Koshkin, V., Saleh, M. C., Sivitz, W. I., Zhang, C. Y., Lowell, B. B., Chan, C. B., and Wheeler, M. B. (2004) *J. Biol. Chem.* **279**, 51049–51056
25. Mitchell, K. J., Tsuboi, T., and Rutter, G. A. (2004) *Diabetes* **53**, 393–400
26. Chan, C. B., MacDonald, P. E., Saleh, M. C., Johns, D. C., Marban, E., and Wheeler, M. B. (1999) *Diabetes* **48**, 1482–1486
27. Gromada, J., Bark, C., Smidt, K., Efanov, A. M., Janson, J., Mandic, S. A., Webb, D. L., Zhang, W., Meister, B., Jeromin, A., and Berggren, P. O. (2005) *Proc. Natl. Acad. Sci. U. S. A.* **102**, 10303–10308
28. Brubaker, P. L., Lee, Y. C., and Drucker, D. J. (1992) *J. Biol. Chem.* **267**, 20728–20733
29. Salapatek, A. M., MacDonald, P. E., Gaisano, H. Y., and Wheeler, M. B. (1999) *Mol. Endocrinol.* **13**, 1305–1317
30. Braunewell, K.-H., and Gundelfinger, E. D. (1997) *Neurosci. Lett.* **234**, 139–142
31. Leung, Y. M., Kang, Y., Gao, X., Xia, F., Xie, H., Sheu, L., Tsuk, S., Lotan, I., Tsushima, R. G., and Gaisano, H. Y. (2003) *J. Biol. Chem.* **278**, 17532–17538
32. Bernstein, H. G., Baumann, B., Danos, P., Diekmann, S., Bogerts, B., Gundelfinger, E. D., and Braunewell, K.-H. (1999) *J. Neurocytol.* **28**, 655–662
33. Ammala, C., Ashcroft, F. M., and Rorsman, P. (1993) *Nature* **363**, 356–358
34. Renstrom, E., Eliasson, L., and Rorsman, P. (1997) *J. Physiol. (Lond.)* **502**, 105–118
35. Harndahl, L., Jing, X. J., Ivarsson, R., Degerman, E., Ahren, B., Manganiello, V. C., Renstrom, E., and Holst, L. S. (2002) *J. Biol. Chem.* **277**, 37446–37455
36. Henquin, J. C. (2000) *Diabetes* **49**, 1751–1760
37. Parsons, T. D., Coorsen, J. R., Horstmann, H., and Almers, W. (1995) *Neuron* **15**, 1085–1096
38. Xia, F., Gao, X., Kwan, E., Lam, P. P., Chan, L., Sy, K., Sheu, L., Wheeler, M. B., Gaisano, H. Y., and Tsushima, R. G. (2004) *J. Biol. Chem.* **279**, 24685–24691
39. Rorsman, P., and Renstrom, E. (2003) *Diabetologia* **46**, 1029–1045
40. Lalli, E., and Sassone-Corsi, P. (1994) *J. Biol. Chem.* **269**, 17359–17362
41. Kushner, J. A., Ciemerych, M. A., Sicinska, E., Wartschow, L. M., Teta, M., Long, S. Y., Sicinski, P., and White, M. F. (2005) *Mol. Cell. Biol.* **25**, 3752–3762
42. Diehl, J. A., Cheng, M., Roussel, M. F., and Sherr, C. J. (1998) *Genes Dev.* **12**, 3499–3511
43. Iype, T., Francis, J., Garmey, J. C., Schisler, J. C., Neshler, R., Weir, G. C., Becker, T. C., Newgard, C. B., Griffen, S. C., and Mirmira, R. G. (2005) *J. Biol. Chem.* **280**, 16798–16807
44. Burgoyne, R. D., O'Callaghan, D. W., Hasdemir, B., Haynes, L. P., and Tepikin, A. V. (2004) *Trends Neurosci.* **27**, 203–209
45. Spilker, C., Gundelfinger, E. D., and Braunewell, K.-H. (1997) *Neurosci. Lett.* **225**, 126–128
46. Malaisse, W. J., Garcia-Morales, P., Dufrane, S. P., Sener, A., and Valverde, I. (1984) *Endocrinology* **115**, 2015–2020
47. Liu, D., Zhen, W., Yang, Z., Carter, J. D., Si, H., and Reynolds, K. A. (2006) *Diabetes* **55**, 1043–1050
48. Kanno, T., Suga, S., Wu, J., Kimura, M., and Wakui, M. (1998) *Pfluegers Arch. Eur. J. Physiol.* **435**, 578–580
49. Kang, G., Chepurny, O. G., and Holz, G. G. (2001) *J. Physiol. (Lond.)* **536**, 375–385
50. Islam, M. S., Leibiger, I., Leibiger, B., Rossi, D., Sorrentino, V., Ekstrom, T. J., Westerblad, H., Andrade, F. H., and Berggren, P. O. (1998) *Proc. Natl. Acad. Sci. U. S. A.* **95**, 6145–6150
51. Yaney, G. C., Civelek, V. N., Richard, A. M., Dillon, J. S., Deeney, J. T., Hamilton, J. A., Korchak, H. M., Tornheim, K., Corkey, B. E., and Boyd, A. E., III (2001) *Diabetes* **50**, 56–62
52. Zhang, X., Odum, D. T., Koo, S. H., Konkright, M. D., Canettieri, G., Best, J., Chen, H., Jenner, R., Herbolsheimer, E., Jacobsen, E., Kadam, S., Ecker, J. R., Emerson, B., Hogenesch, J. B., Unterman, T., Young, R. A., and Montminy, M. (2005) *Proc. Natl. Acad. Sci. U. S. A.* **102**, 4459–4464
53. Kashima, Y., Miki, T., Shibasaki, T., Ozaki, N., Miyazaki, M., Yano, H., and Seino, S. (2001) *J. Biol. Chem.* **276**, 46046–46053
54. Chen, X. L., Zhong, Z. G., Yokoyama, S., Bark, C., Meister, B., Berggren, P. O., Roder, J., Higashida, H., and Jeromin, A. (2001) *J. Physiol. (Lond.)* **532**, 649–659
55. Philippe, J., and Missotten, M. (1990) *J. Biol. Chem.* **265**, 1465–1469
56. Nielsen, D. A., Welsh, M., Casadaban, M. J., and Steiner, D. F. (1985) *J. Biol. Chem.* **260**, 13585–13589
57. Wang, X., Zhou, J., Doyle, M. E., and Egan, J. M. (2001) *Endocrinology* **142**, 1820–1827
58. Petersen, H. V., Serup, P., Leonard, J., Michelsen, B. K., and Madsen, O. D. (1994) *Proc. Natl. Acad. Sci. U. S. A.* **91**, 10465–10469
59. Sherr, C. J. (2000) *Cancer Res.* **60**, 3689–3695
60. Georgia, S., and Bhushan, A. (2004) *J. Clin. Investig.* **114**, 963–968

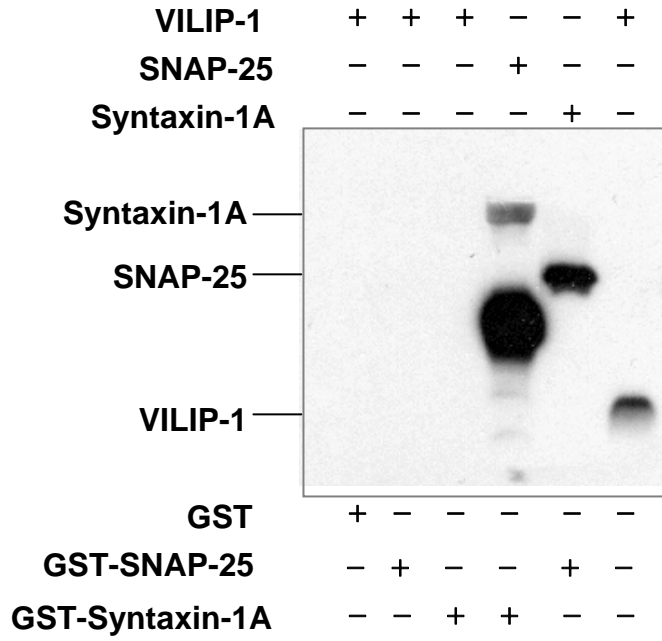
Supplementary Figure 1. VILIP-1-EGFP translocation in HEK293 cells. HEK293 cells transfected with VILIP-1-EGFP were imaged by confocal microscopy within 5 min of treatment with 1mM ionomycin. This image shown is a representation out of three independent experiments.

Supplementary Figure 2. Immunoprecipitation studies with VILIP-1, SNAP-25 and Syntaxin-1A. (A). VILIP-1 interaction with SNAP-25 or Syntaxin-1A. (B). Ponceau-S staining showing the protein loading. The result is representative blot from three independent experiments.

Supplementary Fig. 1.

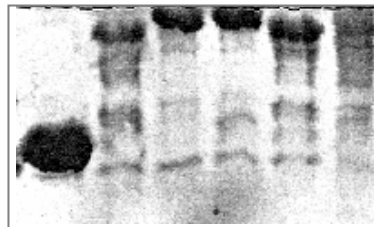


A.



B.

Ponceau-S staining



The Neuronal Ca²⁺ Sensor Protein Visinin-like Protein-1 Is Expressed in Pancreatic Islets and Regulates Insulin Secretion

Feihan F. Dai, Yi Zhang, Youhou Kang, Qinghua Wang, Herbert Y. Gaisano, Karl-Heinz Braunewell, Catherine B. Chan and Michael B. Wheeler

J. Biol. Chem. 2006, 281:21942-21953.

doi: 10.1074/jbc.M512924200 originally published online May 26, 2006

Access the most updated version of this article at doi: [10.1074/jbc.M512924200](https://doi.org/10.1074/jbc.M512924200)

Alerts:

- [When this article is cited](#)
- [When a correction for this article is posted](#)

[Click here](#) to choose from all of JBC's e-mail alerts

Supplemental material:

<http://www.jbc.org/content/suppl/2006/07/28/M512924200.DC1.html>

This article cites 60 references, 31 of which can be accessed free at <http://www.jbc.org/content/281/31/21942.full.html#ref-list-1>